New Multilevel Current-Source PWM Inverter with Full-Bridge Inductor Cells

Toshihiko Noguchi Member (Shizuoka University, ttnogut@ipc.shizuoka.ac.jp)
Suroso Member (University of Jenderal Soedirman, suroso.te.unsoed@gmail.com)

Keywords: current-source inverter, inductor cell, multilevel

This paper proposes a new circuit configuration of a multilevel current-source inverter (CSI). In this new topology, a three-level CSI of which all of the power switches are connected at the identical potential level line works as a main inverter circuit, and inductor cells are connected in parallel with the main inverter as auxiliary circuits. The inductor cells are composed by full-bridge power converters with inductors across the bridges. The inductor cells work to generate intermediate level currents of the output to obtain a multilevel current waveform without any additional external DC power sources.

Fig. 1 shows a schematic diagram of the proposed multilevel CSI. A five-level CSI configuration is obtained by connecting a single inductor cell, a nine-level CSI configuration is achieved by connecting two inductor cells in parallel with the main three-level CSI, and so forth. The relation between the level number of the CSI output current waveform and the number of the inductor cells can be obtained from the equation below:

$$M = 2^{(N+1)} + 1, \cdots\cdots (1)$$

where M is the level number of the output current and N is the number of inductor cells. For M−level CSI, if the DC current sources are assumed to have identical current amplitude I, the current flowing through the N^{th} inductor cell I_{LcN} is expressed as

$$I_{LcN} = \frac{I}{2^N}, \cdots\cdots (2)$$

In the proposed multilevel CSIs, the DC current-sources are indispensable, which can be obtained by employing choppers with smoothing inductors connected with the main three-level inverter. The choppers work as DC current-sources. The choppers consist of two controlled switches that regulate a pair of the DC currents flowing through the two smoothing inductors L_1 and L_2. Fig. 2 shows the concrete five-level CSI configuration with the choppers based DC current-sources. It should be noted that only a single DC voltage source is required and is connected to the CSI. Proportional integral (PI) regulators are independently applied to control two of the DC currents flowing through the smoothing inductors L_1 and L_2, which determine the amplitude of the PWM output current waveform, and the current flowing through the inductor cell L_c.

The operation performance of the proposed multilevel CSI is examined and is validated through some computer simulations. Furthermore, a laboratory experimental prototype of a five-level CSI was set up to verify the proper operation of the proposed new topology. Fig. 3 shows the experimental waveforms of the five-level CSI, i.e., showing the steady state 8-A five-level output current and the load current waveforms. The total harmonic distortion of this five-level output current is 3.3%.

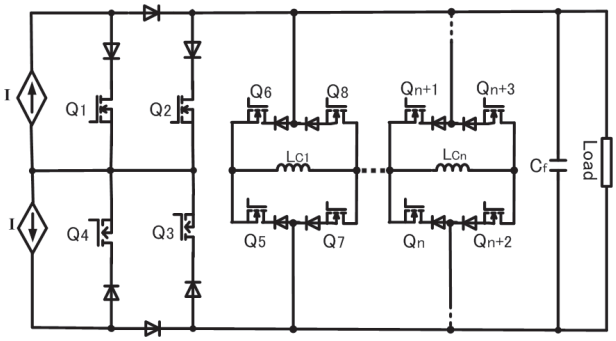

Fig. 1. Generalized configuration of proposed multilevel CSI

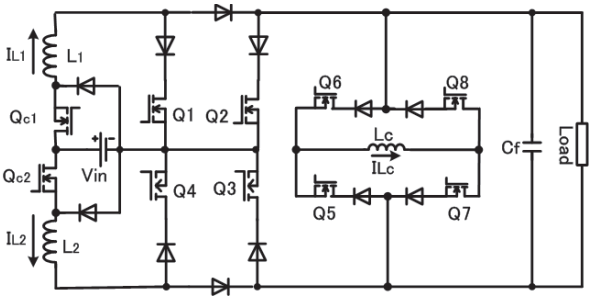

Fig. 2. Five-level CSI with single inductor cell

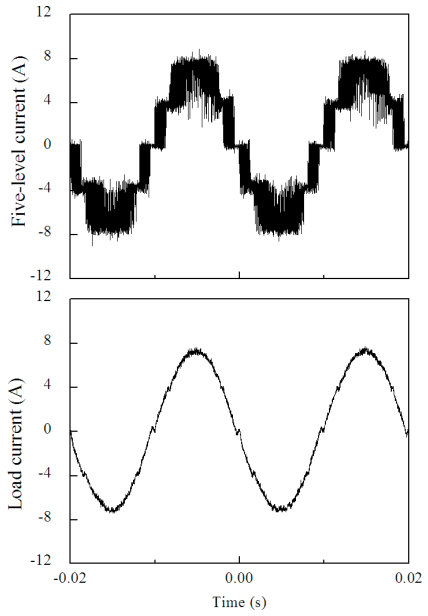

Fig. 3. Experimental waveforms of five-level CSI

Paper

New Multilevel Current-Source PWM Inverter with Full-Bridge Inductor Cells

Toshihiko Noguchi* Member
Suroso**,*** Member

This paper proposes a generalized circuit configuration of a new multilevel current-source inverter (CSI). In this new topology, a three-level CSI of which all the power switches are connected at an identical potential level line works as a main inverter circuit, and inductor cells are connected in parallel with the main inverter as auxiliary circuits. The inductor cells are composed by full-bridge power converters with inductors across the bridges. The inductor cells work to generate intermediate level currents of the output to obtain a multilevel current waveform without any additional external DC power sources. Five-level and nine-level PWM inverter configurations, including their chopper circuits as DC current-power sources, are verified through computer simulations. Furthermore, an experimental prototype of a five-level CSI is setup and is tested. The results show that the circuit works properly to generate the five-level output current waveform, which proves feasibility of the proposed strategy.

Keywords: current-source inverter, inductor cell, multilevel

1. Introduction

The fast ever-lasting development of power devices working at high switching frequencies for medium and high power applications such as metal-oxide-semiconductor field-effect transistors (MOSFETs) and insulated gate bipolar transistors (IGBTs) has improved power converter performance. Development of high-performance semiconductor switches also increases the research interest in high power converters such as multilevel inverters because they have capability to deliver higher output power with low-voltage or low-current rating devices, lower dv/dt and less distorted output waveforms resulting in reduction of the filter size, compared with the conventional two-level inverters [1][3][4].

In general, the inverter topologies can be classified into voltage-source inverters (VSI) and their dual circuits, i.e., current-source inverters (CSI). The VSI has a DC voltage power source and generates AC voltage waveforms to the load, while the CSI delivers AC current waveforms from DC current power sources. The latter features capability of short-circuit protection because of its high-impedance DC power source, but requires protection against an open-circuit to guarantee continuity of the current. The VSI is more widely used than the CSI topology due to some drawbacks such as a heavy inductor used to obtain a smooth DC current and discrete diodes connected in series with the power switches. These drawbacks often degrade the overall efficiency of the CSI [5][7]. However, the series diode might not be necessary because new IGBTs with reverse-blocking capability (reverse-blocking IGBTs) are emerging [6][8]. Furthermore, in order to make the multilevel CSI topology more attractive and affordable, epoch-making ideas to create novel CSI topologies are required.

In this paper, new configurations of the multilevel CSI, applying full-bridge inductor cells, are presented. The inductor cells work to generate the intermediate current-levels through charging and discharging operation modes of the inductors with no additional external DC power sources. The operation performance of the proposed multilevel CSI is examined and is validated through some computer simulations. Furthermore, a laboratory experimental prototype of a five-level CSI was set up to verify proper operations of the proposed new topology, using the power MOSFETs with series blocking diodes.

2. Circuit Configuration and Operation Principle

2.1 Operation Principle of Multilevel CSI Fig. 1(a) shows a basic circuit configuration of a three-level CSI proposed in the authors' previous research work [2]. All of the power switches Q1, Q2, Q3 and Q4 are connected to a common-source (common-emitter) line. Table 1 lists the switching states of this three-level CSI for three-level output current waveform generation of +I, 0 and −I current levels. Furthermore, Fig. 1(b) shows a configuration of a proposed full-bridge inductor cell composed by four controlled power switches Q5, Q6, Q7 and Q8, series blocking diodes and an inductor L_c connected across the bridge.

The newly proposed configuration of the multilevel CSI can be obtained by connecting the former three-level CSI as a main inverter circuit, and a single or more inductor cells as shown in a generalized schematic diagram of the proposed

* Department of Electrical and Electronic Engineering, Shizuoka University
Hamamatsu, Shizuoka 432-8561
** Department of Electrical Engineering, University of Jenderal Soedirman
Purwokerto, Jawa Tengah 53122, Indonesia
*** Department of Energy and Environment Engineering, Nagaoka University of Technology
Nagaoka, Niigata 940-2188

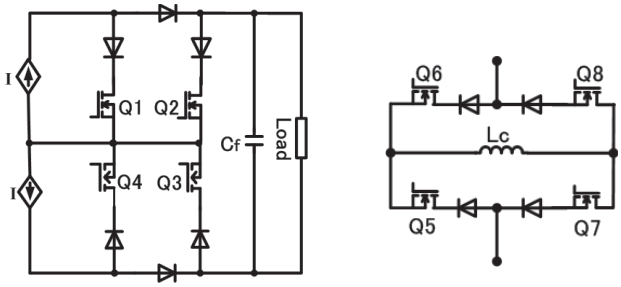

(a) Fundamental three-level CSI (b) Inductor cell

Fig. 1. Three-level CSI and inductor cell

Table 1. Switching states of three-level CSI

Q_1	Q_2	Q_3	Q_4	Output
0	0	1	1	+I
1	0	0	1	0
1	1	0	0	-I

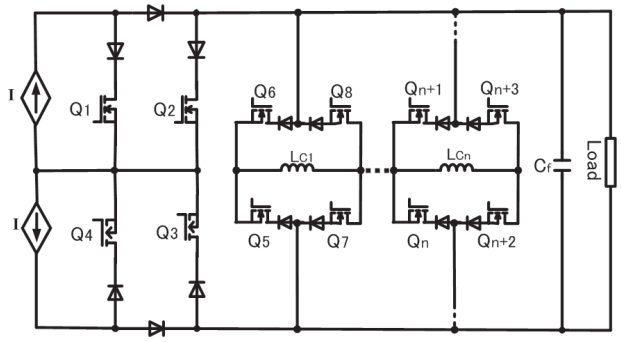

Fig. 2. Generalized configuration of proposed multilevel CSI

multilevel CSI in Fig. 2. The inductor cells are used to generate a multilevel output current from the basic three-level current waveform by controlling charging and discharging operation modes of the inductors.

A five-level CSI configuration is obtained by connecting only a single inductor cell, a nine-level CSI configuration is achieved by connecting two inductor cells in parallel with the main three-level CSI, and so forth. The relation between the level number of the output current waveform and the number of the inductor cells can be expressed as the equation below:

$$M = 2^{(N+1)} + 1, \cdots\cdots (1)$$

where M is the level number of the output current and N is the number of the inductor cells. For M level CSI, if the two DC current-sources are assumed to have identical current amplitude I, the current flowing through the N^{th} inductor cell I_{LcN} is expressed as

$$I_{LcN} = \frac{I}{2^N}, \cdots\cdots (2)$$

Fig. 3 shows an example of a five-level CSI configuration. Furthermore, Fig. 4 shows the operation modes of the inductor cell during a positive cycle operation. Charging operation mode of the inductor L_c is achieved by making the switches Q6 and Q7 turned on, while switches Q5 and Q8 are turned off. A constant current $I_{Lc} = I/2$ flows through the power switches Q6 and Q7 which energizes the inductor L_c to its maximum energy W expressed as

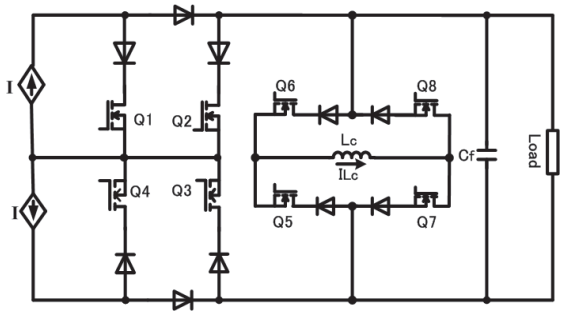

Fig. 3. Five-level CSI with single inductor cell

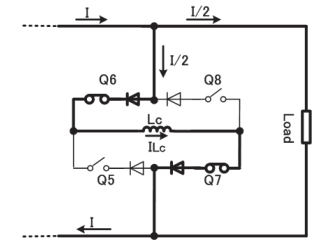

(a) Charging mode of inductor cell

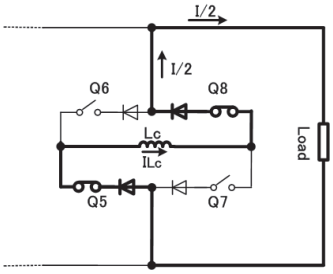

(b) Discharging mode of inductor cell

Fig. 4. Operation modes of inductor cell

$$W = \frac{1}{2} L_c I_{Lc}^2, \cdots\cdots (3)$$

and the discharging operation mode is achieved by turning on the switches Q5 and Q8 and by turning off Q6 and Q7. The stored energy in the inductor is discharged to the load as a current $I/2$. In case of a resistive load, the inductor value can be found as

$$L_c = \frac{I_{Lc} R}{f_s \Delta I_{Lc}}, \cdots\cdots (4)$$

where I_{Lc} is an inductor cell current (A), R is a load resistor (Ω), f_s is a switching frequency of the inductor cell circuit (Hz), and ΔI_{Lc} is an acceptable current ripple of the inductor cell current (A).

Using this new multilevel CSI topology, several advantages can be obtained as follows:

(1) The power switches of the main three-level inverter are connected to an identical potential line; hence they can be driven by using only a single non isolated gate drive power supply.

(2) The level of the output current can be increased by connecting some inductor cell circuits to the main three-level inverter without any additional DC power sources.

(3) All of the inductor cells have the same configuration and allow a simple and modular structure, which

Table 2. Switching states of five-level CSI with inductor cell

Q_1	Q_2	Q_3	Q_4	Q_5	Q_6	Q_7	Q_8	Output
0	0	1	1	1	0	1	0	I
0	0	1	1	0	1	0	1	I
0	0	1	1	0	1	1	0	I/2
1	0	0	1	1	0	0	1	I/2
1	0	0	1	1	0	1	0	0
1	0	0	1	0	1	0	1	0
1	0	0	1	0	1	1	0	-I/2
1	1	0	0	1	0	0	1	-I/2
1	1	0	0	1	0	1	0	-I
1	1	0	0	0	1	0	1	-I

leads to cost reduction in manufacturing process.

The switching state combinations required to generate a five-level current waveform are listed in Table 2 and the more detailed operation modes of the five-level CSI are illustrated in Fig. 5(a) to (g). Power device utility and average switching frequency between Q6Q8 and Q5Q7 in the circulating modes of the inductor cell current are considerations to use redundant switching states for multilevel current generation. It is also related to the heat distribution between the switches Q6Q8 and Q5Q7 caused by their switching and conduction losses. The five output current levels +I, +I/2, 0, −I/2 and −I are generated as follows:

(1) Current level +I

Q1, Q2, Q5 and Q7 are turned off, while Q3, Q4, Q6 and Q8 are turned on, making the currents +I flow to the load;

(2) Current level +I/2

Charging mode: Q1, Q2, Q5 and Q8 are turned off, while Q3, Q4, Q6 and Q7 are turned on, making the currents of +I/2 flow to the load and the inductor cell at the same time. The inductor cell is energized in the charging mode.

Discharging mode: Q2, Q3, Q6 and Q7 are turned off, while Q1, Q4, Q5 and Q8 are turned on, making the stored energy in the inductor be released to the load as a current +I/2. The inductor cell is in discharging mode;

(3) Current level 0

Q1, Q4, Q5Q7 or Q6Q8 are turned on, while Q2, Q3, Q6Q8 or Q5Q7 are turned off, establishing the current circulation for every DC current-source and in the inductor cell. No current flows to the load;

(4) Current level −I/2

Charging mode: Q3, Q4, Q6 and Q7 are turned off, while Q1, Q2, Q5 and Q8 are turned on, making the current −I/2 flow to the load and the inductor cell current is kept at the constant value of I/2. The inductor cell works in the charging mode even though the negative cycle.

Discharging mode: Q2, Q3, Q5 and Q8 are turned off, while Q1, Q4, Q6 and Q7 are turned on, where the stored energy in the inductor is discharged to the load as a current −I/2. The inductor cell is in discharging mode; and

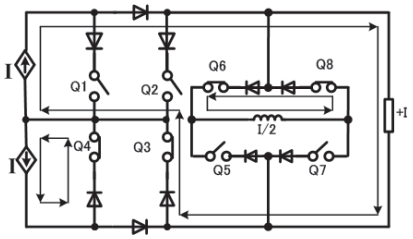

(a) Current +I

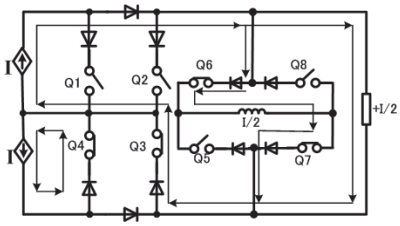

(b) Current +I/2 (charging mode)

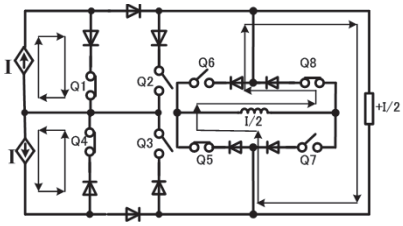

(c) Current +I/2 (discharging mode)

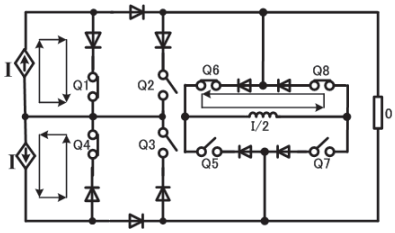

(d) Current 0

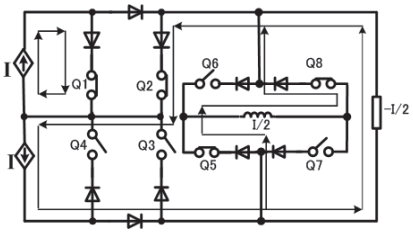

(e) Current −I/2 (charging mode)

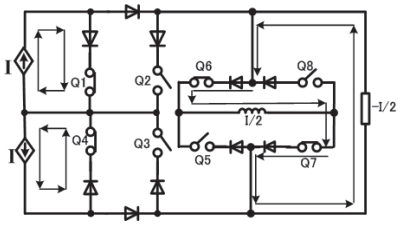

(f) Current −I/2 (discharging mode)

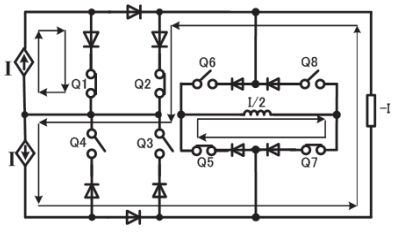

(g) Current −I

Fig. 5. Switching modes for five-level CSI with inductor cell

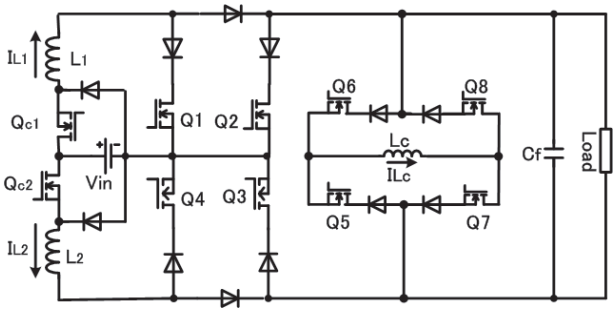

Fig. 6. Five-level CSI with single inductor cell

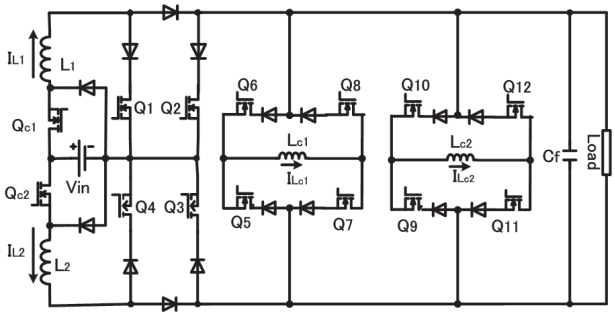

Fig. 7. Nine-level CSI with two inductor cells

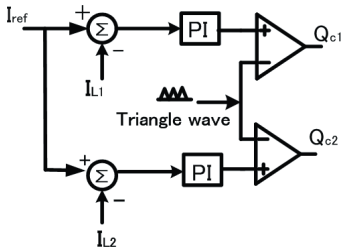

Fig. 8. Control diagram of choppers

(5) Current level −I

Q3, Q4, Q6Q8 or Q5Q7 are turned off, while Q1, Q2, Q5Q7 or Q6Q8 are turned on, making the currents −I flow to the load.

2.2 DC Current Sources In the proposed multilevel CSIs, the DC current sources are indispensable, which can be obtained by employing simple choppers with smoothing inductors connected with the main three-level inverter. The choppers work as DC current sources, which consist of two controlled switches that regulate a pair of the DC currents flowing through the two smoothing inductors L_1 and L_2. Two free-wheeling diodes are used to keep continuous currents flowing through the inductors. Fig. 6 and Fig. 7 show the concrete five-level and nine-level CSI configurations with the choppers based DC current sources. It should be noted that only a single DC voltage source is required and is connected to the CSI.

A control diagram of the choppers for the DC current source is presented in Fig. 8. Proportional integral (PI) regulators are independently applied to control two of the DC currents flowing through the smoothing inductors L_1 and L_2, which determine the amplitude of the PWM output current waveform I_{pwm} simultaneously. Making the inductor currents I_{L1} and I_{L2} follow their reference current I_{ref} is the objective of these current regulators. The switching gate signals

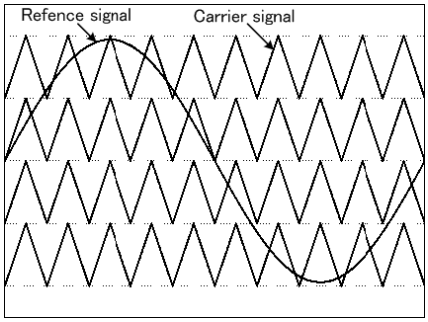

Fig. 9. Multi-carrier based sinusoidal PWM

of the chopper switches are generated by comparing the error signals of the detected steady state inductor currents, and a triangular waveform after passing through the PI regulator. These signals are used to control the duty cycles of the chopper switches to obtain the balanced and stable DC currents.

2.3 PWM Inverter and Inductor Cell Control In order to obtain a low-distortion output current waveform, a pulse width modulation (PWM) technique is applied to the inverter. In this paper, a level-shifted multi-carrier based sinusoidal PWM technique is employed to generate the gate signals for the CSI power switches and to obtain the PWM current waveforms as shown in Fig. 9. All triangular carrier waveforms are in phase with an identical frequency. The frequency of the modulated signal (a reference sinusoidal waveform) determines the fundamental frequency of the output current waveform, while the frequency of the triangular carrier gives the switching frequency of the CSI power switches. An M-level output current waveform using this modulation technique requires (M-1) triangular carriers with DC offsets.

A schematic diagram including the current controller of the inductor cell for the five-level CSI is shown in Fig. 10. The control circuit of the inductor cell functions to switch the operation modes, i.e. charging and discharging modes, of the inductor cell. The current flowing through the inductor I_{Lc} is kept constant. It generates the intermediate level currents based on the output waveform of the main three-level CSI. A PI regulator is applied to zero the error between the detected current flowing through the inductor cell I_{Lc} and the reference current which is half of the main DC currents I_{L1} and I_{L2}. The output of the PI regulator is modulated by a triangular carrier to generate the control signal i[0] determining the operation mode of the inductor cell. In case of the nine-level CSI, the control circuit is similar to the first inductor cell controller mentioned above. The difference is only the reference value for the second inductor cell current I_{Lc2}, which is quarter of the main DC current-source amplitude. Therefore, if there are N inductor cells connected in parallel with the main inverter, the amplitude of the current flowing through the N^{th} inductor cell is as previously expressed in (2).

2.4 Filter Capacitor It is necessary to add a filter capacitor across the load because the inverter works as a current source and the load usually has an inductive component. The filter capacitor also functions to filter the harmonic components, e.g. switching harmonic components, of the PWM multilevel output current. The harmonic components of the PWM current should flow into the filter C_f. In general, the parasitic resistor component of the capacitor is much lower

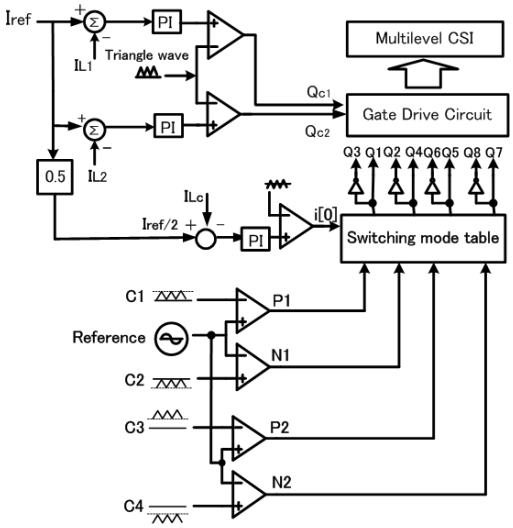

Fig. 10. Control diagram of five-level CSI with inductor cell

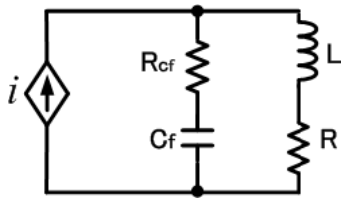

Fig. 11. Schematic diagram of CSI, filter C_f and load

Table 3. Test parameters

Inductors in power sources and inductor cell	1.6 mH and 5 mH
Power source voltage	160 V
Inverter switching frequency	22 kHz
Filter capacitor C_f	5 μF
Load	$R = 6\ \Omega$, L =1.2 mH
Output current frequency	50 Hz

than the load resistance; hence the losses and heat caused by the harmonic components flowing into the filter capacitor are much smaller. Moreover, using the higher switching frequency with its constraints, and with the higher level number of the output current, a smaller size of the filter capacitor is applicable. A proper choice of the capacitor is important to minimize the heat in the filter, e.g. capacitor with small equivalent series resistance (ESR).

Fig. 11 shows a circuit diagram of a CSI connected with the filter capacitor (C_f) with its internal resistor (R_{Cf}), and the load (R and L). The equivalent impedance of this circuit is expressed as

$$Z_{eq} = \frac{(R + j\omega L)\left(R_{cf} - j\dfrac{1}{\omega C_f}\right)}{(R + R_{cf}) + j\left(\omega L - \dfrac{1}{\omega C_f}\right)}. \quad \cdots\cdots (5)$$

For this circuit, the resonance frequency (ω_o) can be found as

$$\omega_0 = \frac{1}{\sqrt{LC_f}}\left[\frac{R^2C_f - L}{R_{cf}^2C_f - L}\right]^{\frac{1}{2}}. \quad \cdots\cdots (6)$$

This capacitor value should be avoided in order to prevent such resonance in the circuit. In addition, as in dual property with the voltage source inverter, since the inverter behaves as a current source, it should be connected with a capacitive load (including the filter capacitor). Thus, the total impedance connected to the CSI as expressed in (5) should be a capacitive. It is another key in choosing the value of the

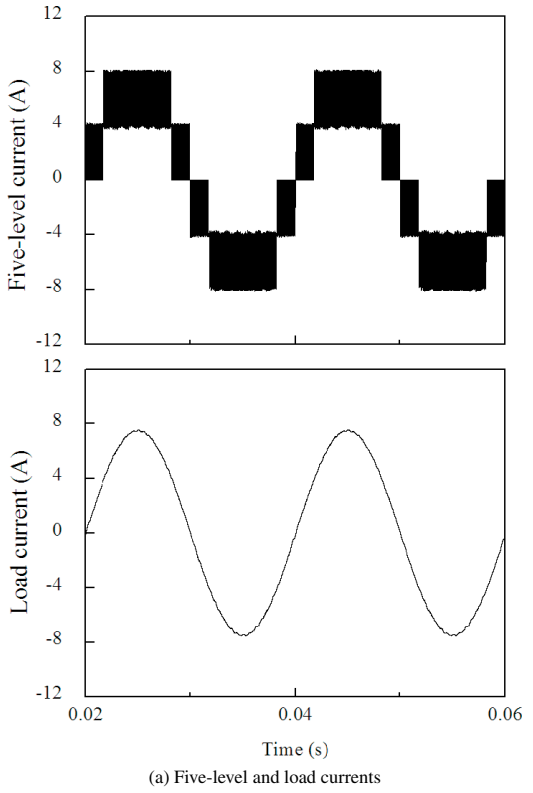

(a) Five-level and load currents

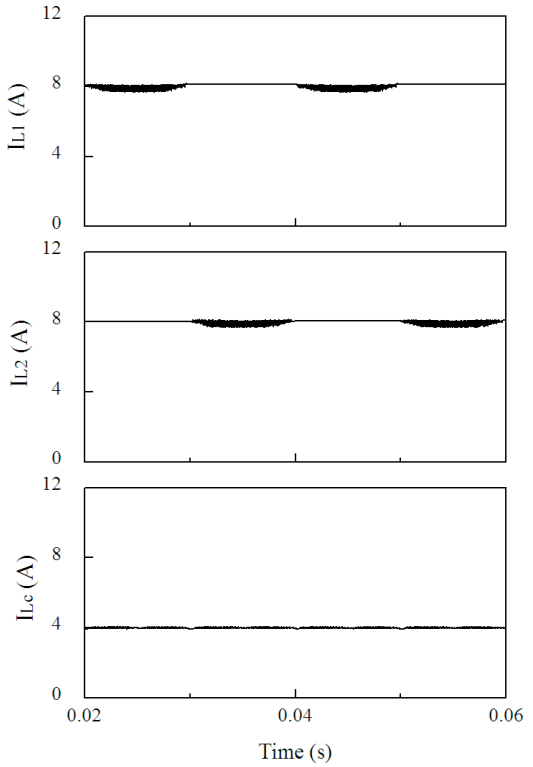

(b) Waveforms of DC current sources I_{L1}, I_{L2} and inductor cell current I_{Lc}

Fig. 12. Simulation result of five-level CSI

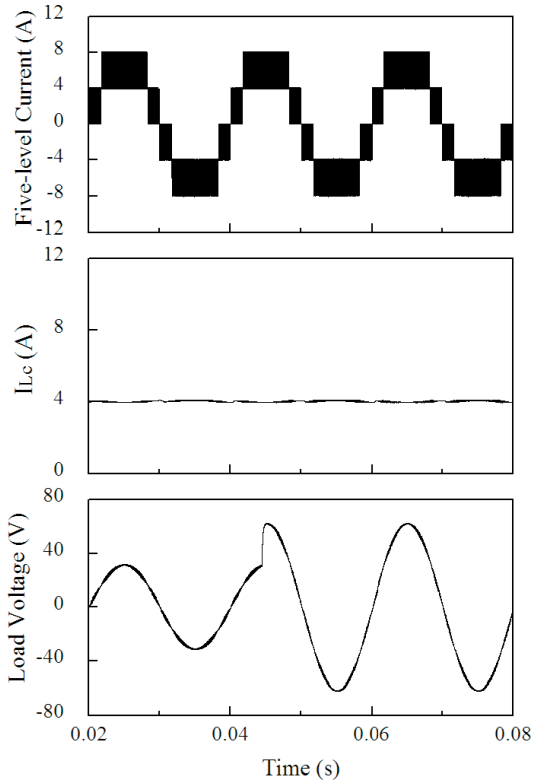

Fig. 13. Test result of load step change in five-level CSI (from 4 Ω to 8 Ω)

filter capacitor.

3. Computer Simulation Results

In order to test the operation of the proposed multilevel CSI topology, computer simulations are conducted by using a PSIM software. This section presents the computer simulation results of the proposed five-level and nine-level CSI configurations. The simulation parameters are listed in Table 3. The five-level and nine-level configurations shown in Fig. 6 and Fig. 7 are tested with a single DC power source.

Fig. 12(a) shows a computer simulation result of the five-level CSI, where the five-level and the load current waveforms are presented. Fig. 12(b) shows the current waveforms flowing through inductors L_1, L_2 and L_c. The amplitude of the DC current sources are well balanced for both smoothing inductors I_{L1}, I_{L2}, and the current amplitude of the inductor cell I_{Lc} corresponds to half of the peak level of the five-level output current waveform. Fig. 13 shows the test result of a load step change from 4 Ω to 8 Ω showing the five-level current, inductor cell current and load voltage waveforms at constant output current and constant gains of PI controller.

Furthermore, Fig. 14(a) shows another computer simulation result of the nine-level CSI. Fig. 14(b) shows the DC current sources I_{L1} and I_{L2}, and the first and the second inductor cell current waveforms I_{Lc1} and I_{Lc2} of the nine-level CSI. The amplitude of the DC current sources are also well balanced for both smoothing inductors, and the amplitudes of inductor cell current waveforms I_{Lc1} and I_{Lc2} are correspond to half and quarter of the peak level of the nine-level output current waveform, respectively. It is confirmed that the five-level and the nine-level CSIs can generate proper multilevel current waveforms.

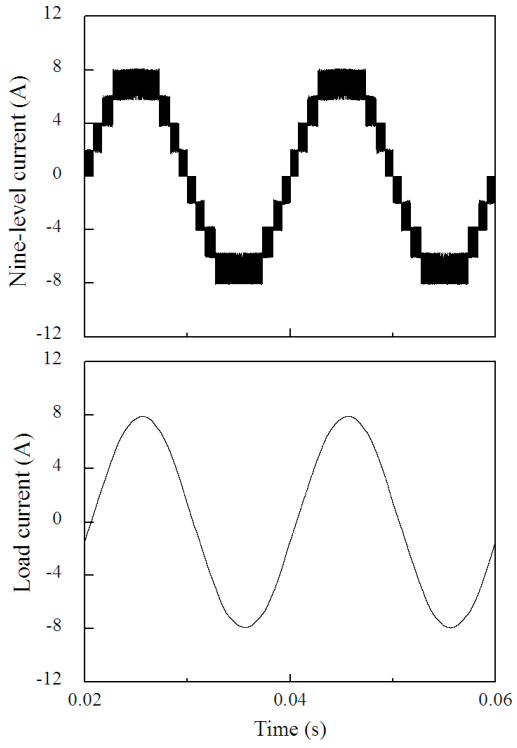

(a) Nine-level and load currents

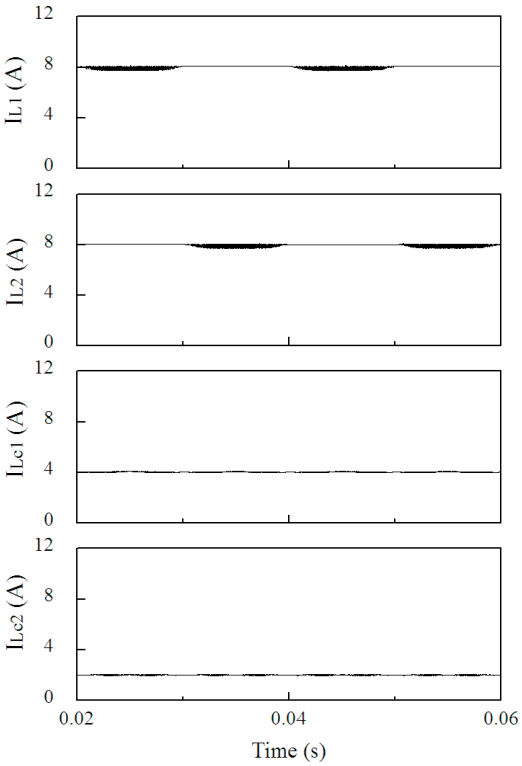

(b) Waveforms of DC current sources I_{L1}, I_{L2} and inductor cell currents I_{Lc1}, I_{Lc2}

Fig. 14. Simulation result of nine-level CSI

4. Experimental Test Results

In order to verify and to prove feasibility of the proposed multilevel CSI configuration experimentally, a laboratory prototype of the five-level CSI was constructed with

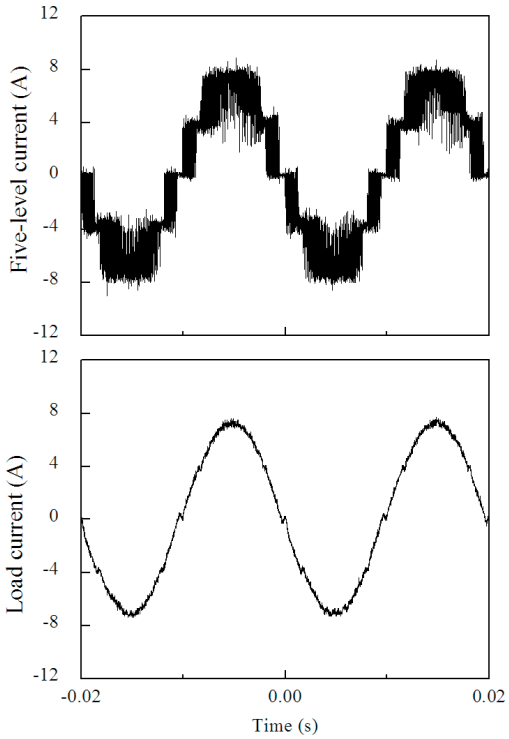

Fig. 15. Experimental result of five-level and load currents

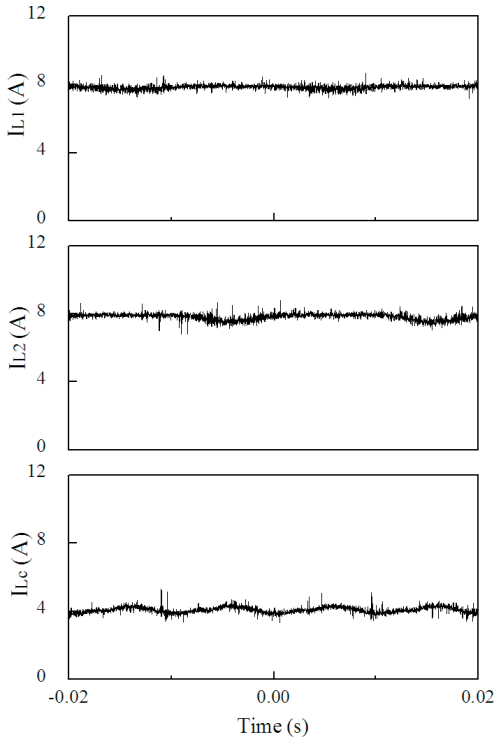

Fig. 16. Experimental result of DC current sources I_{L1}, I_{L2} and inductor cell current I_{Lc}

power MOSFETs (FK30SM-5) and fast recovery diodes (HFA16PB120). The implemented circuit specifications are identical as the computer simulation parameters in Table 3.

Fig. 15 shows experimental waveforms of the five-level CSI, i.e., a steady state 8-A five-level output current and a load current waveforms. Fig. 16 shows the current waveforms flowing through inductors L_1, L_2 and L_c. The inverter works properly generating a five-level output current waveform. As can be seen in the figure, a low distorted sinusoidal load current waveform is also obtained after filtering by a small 5-μF filter capacitor. All of the experimental waveforms agree with those of the computer simulation results. The ripple difference between the DC input current I_{L1} and I_{L2} is caused by the difference in the delivering periods of the current to the load. In one cycle, a current source supplies for only half cycle of the current to the load. The rest of the cycle is a current circulation mode. In addition, the diodes and power MOSFETs switches used in the experimental setup have relatively high forward voltage drop and high on-resistance, which introduce a problem in controlling the inductor cell current, and cause more ripple in the inductor cell current. Using higher-performance diodes and power MOSFETs, the ripple of the inductor cell current can be reduced. Fig. 17 shows a frequency analysis result of the five-level PWM output current waveform including the switching harmonic component and its sidebands, with total harmonic distortion (THD) of 3.3%. Fig. 18 shows a frequency spectrum of load current presenting elimination and reduction of the harmonic components with a small 5-μF filter capacitor.

Fig. 19 shows an efficiency characteristic of the prototype five-level CSI. As can be seen, the efficiency is low in a light load condition which is caused by conduction losses of the inductors and switching devices becoming relatively dominant

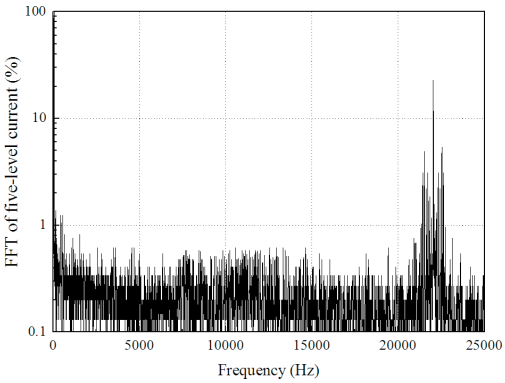

Fig. 17. FFT of five-level output current

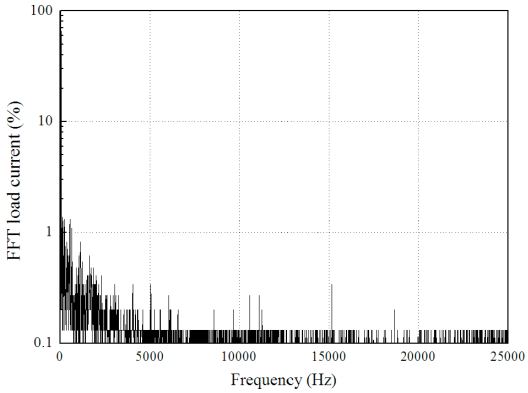

Fig. 18. FFT of load current

against the load power. In general, this is a substantial drawback of current-source power converters. However, the efficiency increases as the load becomes heavier, and the maximum efficiency of the prototype was confirmed to be 87.8%

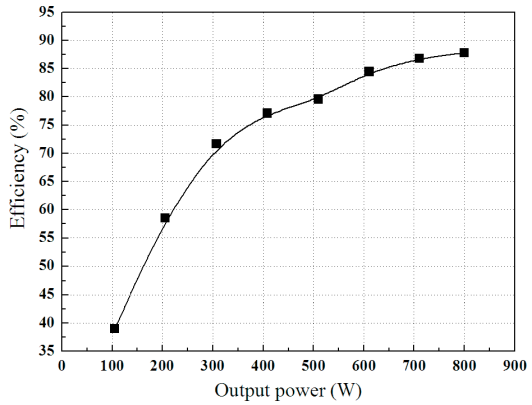

Fig. 19. Efficiency characteristic of five-level CSI

at the load of 0.8 kW.

5. Conclusion

In this paper, a new generalized configuration of a multilevel CSI, which employs auxiliary full-bridge inductor cells has been proposed. A multilevel current waveform is obtained by controlling the charging and the discharging operation modes of the inductor cells connected in parallel with the main three-level CSI. The validity of the proposed topology has been verified through computer simulations and in an experimental setup.

(Manuscript received Nov. 3, 2009,
revised Feb. 17, 2010)

References

(1) P.G. Barbosa, H.A.C. Braga, M.C. Barbosa, and E.C. Teixeria: "Boost Current Multilevel Inverter and Its Application on Single Phase Grid Connected Photovoltaic System", *IEEE Trans. Power Electronic*, Vol.21, No.4, pp.1116–1124 (2006-7)

(2) Suroso and T. Noguchi: "Three-level Current-Source PWM Inverter with No Isolated Switching Devices for Photovoltaic Conditioner", *IEEJ Trans. Industry Application*, Vol.129, No.15, pp.505–510 (2009)

(3) F.L.M. Antunes, A.C. Braga, and I. Barbi: "Application of A Generalized Current Multilevel Cell to Current Source Inverters", *IEEE Trans. Power Electronic*, Vol.46, No.1, pp.31–38 (1999-2)

(4) J. Rodiguez, J.S. Lai, and F.Z. Peng: "Multilevel Inverter: A Survey of Topologies, Controls, and Application", *IEEE Trans. Industrial Electronics*, Vol.49, No.4, pp.724–738 (2002-8)

(5) B.P. McGrath and D.G. Holmes: "Natural current Balancing of Multicell Current Source Inverter", *IEEE Trans. Power Electronic*, Vol.23, No.3, pp.1239–1246 (2008-5)

(6) C. Klumpner and F. Blaajerg: "Using Reverse Blocking IGBTs in Power Converters for Adjustable-Speed Drives", *IEEE Trans. Inductry Applications*, Vol.42, No.3, pp.807–816 (2006-5/6)

(7) S. Kwak and H.A. Toliyat: "Multilevel Converter Topology Using Two Types of Current-Source Inverters", *IEEE Trans. Inductry Applications*, Vol.42, No.6, pp.1558–1564 (2006-11/12)

(8) C. Liu, D. Xu, and L. Jun: "Three-phase Current-Source Buck Type PFC Converter with Reverse-Blocking IGBTs", *Power Electronics Specialist Conference*, pp.1331–1335 (2007)

Toshihiko Noguchi (Member) was born in 1959. He received the B.Eng. degree in electrical engineering from Nagoya Institute of Technology, Nagoya, Japan, and the M.Eng. and D.Eng. degrees in electrical and electronics systems engineering from Nagaoka University of Technology, Nagaoka, Japan, in 1982, 1986, 1996, respectively. In 1982, he joined Toshiba Corporation, Tokyo, Japan. He was a Lecturer at Gifu National College of Technology, Gifu, Japan, from 1991 to 1993 and a Research Associate in electrical and electronics systems engineering at Nagaoka University of Technology from 1994 to 1995. He was an Associate Professor at Nagaoka University of Technology from 1996 to 2009. He has been a Professor at Shizuoka University since 2009. His research interests are static power converters and motor drives. Dr. Noguchi is a Senior Member of the IEEE.

Suroso (Member) was born in 1978. He received the B.Eng. degree in electrical engineering, from Gadjah Mada University, Indonesia in 2001 and the M.Eng. degree in electrical engineering from Nagaoka University of Technology, Japan in 2008. He is a Lecturer at electrical engineering department, University of Jenderal Soedirman, Purwokerto, Jawa Tengah, Indonesia. He is currently a doctor student at energy and environment engineering department, Nagaoka University of Technology, Japan. His research interest includes power electronics and its application in renewable energy technology. He is a student member of the IEE-Japan and the IEEE.